

# Rspo3 regulates abnormal differentiation of small intestinal epithelial cells in diabetic state

Ti-Dong Shan (✉ [shantidong26@163.com](mailto:shantidong26@163.com))

First Affiliated Hospital of Qingdao University

Yue Han

Qingdao University Medical College

Xue-Guo Sun

Qingdao University

Yue-Ping Jiang

Qingdao Medical College: Qingdao University Medical College

Li Chen

Qingdao University

---

## Research Article

**Keywords:** diabetes mellitus, Rspos, microRNA, intestinal epithelial stem cell, differentiation

**Posted Date:** March 4th, 2021

**DOI:** <https://doi.org/10.21203/rs.3.rs-265005/v1>

**License:**   This work is licensed under a Creative Commons Attribution 4.0 International License.

[Read Full License](#)

---

# Abstract

**Objective:** The problems caused by diabetes mellitus (DM) related complications are the focus in clinical treatment. However, little is known about diabetic enteropathy (DE) and its the potential underlying mechanism.

**Methods:** Intestinal cells (IEC) and Intestinal stem cells (IESC) obtained from BKS.Cg-Dock7<sup>m+/+</sup>Lepr<sup>db</sup>/JNju (DM) mice were used to detect Rspo3 by RT-qPCR, western blotting, Immunohistochemistry, and immunofluorescence. The role of Rspo3 in the abnormal differentiation of IECs of DM was clarified by knockout experiments. Through miRNA expression profiles, bioinformatic analysis, and RT-qPCR, we further analyzed differentiation related miRNA from IECs in DM mice.

**Results:** The abnormal differentiation of small intestinal epithelial cells (IECs) was found in DM state. The expression of R-spondin 3 (Rspo3) was upregulated in IECs of DM state. And this phenomenon was associated with R-spondin 3 (Rspo3) overexpression. Additionally, Rspo3 is a major determinant of Lgr5+ stem cell identity upon DM state. Microarray analysis, Bioinformatics analysis and luciferase reporter assays revealed that microRNA (miR)-380-5p was directly targeted Rspo3. Moreover, miR-380-5p upregulation was observed to attenuate the abnormal differentiation of IECs through Rspo3 expression.

**Conclusion:** Together, our results provide definitive evidence for the essential role of Rspo3 in differentiation of small intestinal epithelial cells (IECs) in DM state.

## Introduction

Diabetes mellitus (DM) is defined as a very common metabolic disorder, and the related complications caused by it cause damage to the health of millions of people worldwide [1]. Since diabetes-related complications have become the main cause of death worldwide, learning its pathogenesis has become an important and long-term problem in medical research. Although important progress has been made, there are still many discoveries that require further study [2]. Previous studies have shown that diabetic enteropathy (DE) is mainly a functional change caused by diabetic autonomic neuropathy, but later other precipitating factors, such as inflammation and microbiota, have been recognized [3]. However, abnormally differentiated intestinal cells (IEC) as an early change of phenotype has caused people to have a new understanding of DE. In our previous research, we found that the abnormal proliferation of IECs was found in diabetic mice [4]. So, the mechanism in abnormal differentiation of IECs is the focus in this study. Studies have confirmed that the development of colorectal cancer was highly associated with DM [5, 6], supporting the hypothesis that the association between the abnormal differentiation of IECs and DM.

Intestinal stem cells (IESC) undergo dynamic differentiation from crypts to villi every 3–10 days. Study have found that the Lgr5 + crypt cells act as stem cells that reside at the crypt base regenerated normal IECs during homeostasis and are essential during regeneration [7]. Wnt signal pathway is a critical component of Lgr5 + crypt cells. In details, The continuous activation of Wnt pathway in IESC causes

excessive activation of  $\beta$ -catenin, which is sufficient to induce IEC polyposis and even cancer [8]. Structurally, (Rspo1-4) are unified by a common domain architecture comprising a C-terminal Thrombospondin type 1 repeat domain and two furin-like repeats, where the latter is essential for their function in enhancing Wnt signaling [9]. R-spondin proteins (Rspo1-4) are secreted amplifiers in Wnt signal among animals. Sources of Wnt amplifiers Rspos are elucidated their functional contribution in intestinal homeostasis [10]. Given the crucial roles of Rspos in self-renewal IECs, Rspos function and underlying mechanism in DE has provided new insight in this study.

MicroRNA (miRNA) is a conserved non-coding RNA composed of approximately 18 to 22 nucleotides in length [11]. MiRNAs degrades or inhibits its message RNA (mRNA) expression by directly binding its 3'-untranslatable region (3'-UTR). MiRNA interacts closely with cell proliferation, differentiation, apoptosis and differentiation. Abnormal miRNA can be expressed to cause the pathophysiological process of various cancers. However, its role in IECs of DM remains largely unclear and need to be study.

In this study, we investigated the role of RSPOs in abnormal IEC differentiation of DM state, miRNA microarray and bioinformatic analysis was used to identify candidate miRNAs associated with abnormal differentiation of IECs in DM mice, to characterize a mechanism for RSPOs in abnormal IEC differentiation.

## Materials And Methods

### Mice

BKS.Cg-Dock7<sup>m</sup>+/+Lepr<sup>db</sup>/JNju (db/db) mice and identical genetic background BKS heterozygote db/+ mice were all obtained from the Model Animal Research Center of Nanjing University (Jiangsu, China). 16-week-old homozygous mice were housed individually in sterile microisolators for the duration of the experiment. The db/db mice were maintained for 8 weeks with hyperglycemia (random blood glucose level  $\geq 16.7$  mmol/l). db/+ mice (random blood glucose level  $< 11.1$  mmol/l) were used as the controls [12].

All experimental procedures were performed by the Animal Care Committee of Qingdao University.

### Reverse transcription-quantitative PCR (RT-qPCR) analysis

Total RNA was extracted from cell lines and tissue samples with a TRIzol reagent (Invitrogen; Thermo Fisher Scientific, Inc.) following the manufacturer's manual. Then, RT-qPCR was performed with PrimeScript<sup>™</sup> RT Master mix and qPCR SYBR<sup>®</sup> Premix Ex Taq<sup>™</sup> (Takara Biotechnology Co., Ltd.). The following thermocycling conditions were used for qPCR: denaturation at 95°C for 7 min; followed by 40 cycles of denaturation at 95°C for 15 sec and 60°C for 1 min. miRNA levels were performed by SYBR PrimeScript<sup>™</sup> miRNA RT-PCR kit (Takara Biotechnology Co., Ltd.). The following primers were used in Table 1. The RNA levels were calculated using the the 2-Cq $\Delta\Delta$  method [13].

### Bioinformatics analysis

MiRNAs potentially bind to the 3'UTR of Rspo mRNA were predicted using 2 different algorithms between TargetScan 7.2 (<http://www.targetscan.org/>) and miRanda (<http://www.miranda.org>).

### **Culture of cell lines**

293T cells were obtained from American Type Culture Collection and were cultured in DMEM (Invitrogen; Thermo Fisher Scientific, Inc.) supplemented with 10% FBS (Gibco; Thermo Fisher Scientific, Inc.), and 1% penicillin/streptomycin and streptomycin (0.1 mg/ml; Sigma-Aldrich; Merck KGaA) at 37°C with 5% CO<sub>2</sub>.

### **Primary IEC isolation**

The small intestine was dissected out from mice to expose the crypts and villi through sliced longitudinally. All procedures as described previously [12, 14, 15, 16].

### **Cell transfection**

The siRNAs targeting Rspo3, miRNA mimic (agomiR-380-5p) and inhibitor (antagomiR-380-5p) were synthesized and purchased from Guangzhou RiboBio Co., Ltd. (China). Cells ( $2 \times 10^5$  cells/well) were plated into six-well plates and incubated overnight prior to transfection. At 40–60% confluence, cells were transfected with siRNAs (15 nM), miRNA mimic (15 nM) or inhibitor (15 nM) into cells using Lipofectamine 3000 (Invitrogen; Thermo Fisher Scientific, Inc.).

### **Dual-luciferase reporter plasmid transfection**

The wild-type (WT) or mutant-type (MUT) of the 3'UTR of Rspo3 sequences was cloned into the pmiR-RB-REPORT™ plasmid (Guangzhou RiboBio Co., Ltd., Guangzhou, China). After incubation for 48 h, the cells were collected and firefly and Renilla luciferase activity were measured using the Dual-Luciferase Reporter Assay system (Promega Corporation, Madison, WI, USA). Firefly luciferase activity was normalized to Renilla luciferase activity. The luciferase efficiency was evaluated at 2 min following Stop & Glo® reagent using SpectraMAX Multifunctional Microplate Reader (Molecular Devices).

### **Downregulating the expression of Rspo3 in vivo**

Mice were randomly divided into four groups, with 24 in each group. All mice received a tail vein injection once a day for 3 days. The db/+NS group comprised control mice receiving saline (0.9%; same volume as the experimental group) injections [14, 15, 17, 18], and the db/db-NS group comprised DM mice receiving saline (0.9%; same volume as the experimental group) injections [14, 15, 17, 18]; the db/db-si-Rspo3 mice received injections of Rspo3 siRNA (80 mg/kg body weight, 14,15, 17,18), and the db/db-agmiR-380-5p mice received injections of agmiR-380-5p (80 mg/kg body weight, 14,15, 17,18). In each group, six mice were euthanized with an intraperitoneal injection of ketamine/xylazine (100/10 mg/kg body weight) on day 0 (prior to injection), day 2, day 4, and day 6 for further study.

### **In situ hybridization**

A DIG-labeled LNA-miR-380-5p probe was synthesized following the manufacturer's instructions by RiboBio (Guangzhou, China.) In brief, a 5-mm section of paraffin-embedded tissues was incubated with methanol in PBST solution, then fixed with 4% formaldehyde solution and washed with SSC buffer, and then permeabilized with Triton X-100 solution. The tissues was incubated with DIG-labeled LNA-miR-380-

5p probe for hybridization at 37°C overnight. Then, miR-380-5p expression was determined using diaminobenzidine solution (1:900; Boster Biological Technology), following the staining intensity was observed using a microscope BX51 (Olympus Corporation). The staining was quantified by counting the number of positive cells at a magnification of x400.

### **Immunohistochemistry and immunofluorescence.**

The paraffin-embedded mice tissue samples were sectioned at a thickness of 5 µm sections. The sections were deparaffinized in xylene and rehydrated in an ethanol gradient. Tissue sections was quenched by a peroxidase-blocking solution (Dako), and then incubated in milk for 5 min, and overnight at 4°C with primary antibodies, including anti-SI antibody (1:100; cat no. ab84977), anti-Tff3 antibody (1:150; C cat no. sc398651), anti-Lyz1 antibody (1:150; cat no. ab189937), anti-ChgA antibody (1:100; cat no. ab15160), anti-Rspo1 antibody (1:200; cat no. ab106556), anti-Rspo2 antibody (1:100; cat no. ab132836), anti-Rspo3 antibody (1:150; cat no. ab233113), anti-Rspo4 antibody (1:100; cat no. ab189515), and anti-β-actin antibody (1:100; cat no. ab8226) (all from Abcam, Inc.).

For immunohistochemistry, the section was incubated with anti-HRP rabbit/mouse secondary antibody (Dako, Glostrup, Denmark) at room temperature for 2h, and color developed by DAB (Dako). The sections were stained with Mayer's hematoxylin solution and dehydrated by xylene, and mounted under a microscope.

For immunofluorescence, the section was incubated with Alexa Fluor 488 conjugated anti-rabbit (1:1000; cat no. 4412; CST) and 546 conjugated anti-mouse (1:1000; cat no. A11030; Thermo) secondary antibody after the primary antibody. The nucleus was stained DAPI (1:5000; cat no. D8417; Sigma, D8417). And the fluorescent pictures were detected by the FV1200 laser scanning microscope (Olympus).

### **Protein extraction and western blotting**

Total protein from tissues was using RIPA Buffer (Thermo Fisher Scientific, Inc.) supplemented with protease inhibitor cocktail (Roche Applied Science). Protein samples (40 µg/sample) for each group was loaded and resolved on a 10% SDS-PAGE gels, and subsequently transferred to the polyvinylidene fluoride (PVDF) membranes membrane (EMD Millipore). Then, the membranes were blocked with 5% skim milk at room temperature for 1 h and incubated at 4°C overnight with primary antibodies: anti-SI antibody (1:400; cat no. ab84977), anti-Tff3 antibody (1:400; C cat no. sc398651), anti-Lyz1 antibody (1:250; cat no. ab189937), anti-ChgA antibody (1:200; cat no. ab15160), anti-Rspo1 antibody (1:1,000; cat no. ab106556), anti-Rspo2 antibody (1:1,000; cat no. ab132836), anti-Rspo3 antibody (1:1,000; cat no. ab233113), anti-Rspo4 antibody (1:1,000; cat no. ab189515), and anti-β-actin antibody (1:1,000; cat no. ab8226) (all from Abcam, Inc.). The blots were incubated with the horseradish peroxidase-conjugated secondary antibodies (cat no. 7074S; Cell Signaling Technology, Inc.) at 37°C for 1 h at room temperature and visualized using an enhanced chemiluminescence Ultra Western HRP Substrate kit (cat no. WBULS0100; EMD Millipore). Signals were analyzed by Quantity One software version 4.6.2 (Bio-Rad Laboratories, Inc.) and the intensity values were normalized to β-actin.

### **Statistical analysis**

Results data are represented as the mean  $\pm$  standard deviation and analyzed using the statistical software package (SAS 8.0 for Windows; SAS Institute, Inc., Cary, NC, USA). Comparisons between groups were analyzed with a Student's test, and one-way ANOVA with Tukey's post hoc test used for multiple group comparisons.  $P < 0.05$  was considered as the criterion for statistical significance.

## Results

### Abnormal differentiation of IECs in DM state

Sucrase-isomaltase (SI), trefoil factor 3 (Tff3), lysozyme 1 (Lyz1), and chromogranin A (ChgA) were used as markers for absorptive cells, goblet cells, Paneth cells, and endocrine cells, respectively. In this study, RT-qPCR analysis revealed that the IECs in db/db mice have an abnormal differentiation profile compared with db/+. The results found that the overexpression of SI, Tff3, Lyz1 when compared with db/+ mice ( $n = 6$ ,  $p < 0.05$ ; Fig. 1a), however, the low expression of ChgA ( $n = 6$ ,  $p < 0.05$ ; Fig. 1a). Western blot analysis was also used to investigate protein expression levels (Fig. 1b). The protein expression of SI, Tff3, and Lyz1 was significantly increased, and ChgA was decreased in db/db mice ( $n = 6$ ,  $p < 0.05$ ; Fig. 1c). Meantime, the immunohistochemistry showed the numbers of SI-, Tff3-, and Lyz1-positive cells in db/db mice were significantly upregulated, and the downregulated numbers of ChgA-positive cells compared with db/+ mice ( $n = 6$ ,  $p < 0.05$ ; Fig. 1d,1e). Taken together, these results suggest that abnormal differentiation of IECs in DM mice.

### Rspo3 is overexpressed in the IECs of DM state.

To study the role of four Rspo family members in the IECs of DM state, their expression profiles were detected in db/db mice. Subsequently, RT-qPCR analysis showed that Rspo3 showed a higher expression among them in the IECs of db/db mice than db/+ mice ( $n = 6$ ,  $p < 0.05$ ; Fig. 2a). Rspo3 protein levels were also significantly upregulated in the IECs of db/db mice ( $n = 6$ ,  $p < 0.05$ ; Fig. 2b, 2c). As shown by Immunohistochemistry, we found that Rspo3 expression predominantly localized in the stromal compartment that surrounds the crypt base. And, the expression of Rspo3 in db/db mice was significantly increased ( $n = 6$ ,  $p < 0.05$ ; Fig. 2d, 2e). Overall, we hypothesized that Rspo3 plays an important role in the abnormal differentiation of IECs in DM mice.

### Abnormal differentiation of IECs in DM state is associated with overexpressed Rspo3

Rspo3 expression in IECs from stableTM si-Rspo3 treated db/db mice was significant reduction in 2, 4 and 6 days compared to db/db mice ( $n = 6$ ,  $p < 0.05$ ; Fig. 3a); and the expression of Rspo3 on the 4th day after administration was similar to that in db/+ mice ( $n = 6$ ,  $p > 0.05$ ; Fig. 3a). On the 4th day after stableTM si-Rspo3 administration, the increased mRNA expression of SI, Tff3, and Lyz1 was inhibited in db/db mice, and ChgA mRNA expression was increased ( $n = 6$ ,  $p < 0.05$ ; Fig. 3b). This phenotype was further confirmed by Western blot, protein expression of SI, Tff3, and Lyz1 in si-Rspo3 administration db/db mice was significantly decreased and close to the levels observed in db/+ mice ( $n = 6$ ,  $p < 0.05$ ; Fig. 3c, 3d). Furthermore, downregulated ChgA protein expression in db/db mice was partially normalized after si-Rspo3 administration compared with db/+ mice ( $n = 6$ ,  $p < 0.05$ ; Fig. 3c, 3d). Moreover, after si-

Rspo3 administration in db/db mice, the numbers of Sl-, Tff3-, and Lyz1-positive cells were significantly decreased, and the decreased numbers of ChgA-positive cells observed were normalized ( $n = 6$ ,  $p < 0.05$ ; Fig. 3e, 3f). These results suggest that Rspo3 might be capable of promoting abnormal differentiation of IECs in DM mice.

### **RSPO3 expands Lgr5 + stem cells in DM state**

As shown in Fig. 4a, RT-qPCR analysis revealed that Lgr5 in db/db-NS mice showed the higher expression compared with db/+NS mice ( $n = 6$ ,  $p < 0.05$ ; Fig. 4a). And, Lgr5 protein levels were also significantly upregulated by Western blot ( $n = 6$ ,  $p < 0.05$ ; Fig. 4b, 4c). Immunohistochemistry was found that Lgr5 expression was predominantly localized in crypt of IECs and had expansion expression of Lgr5 + stem cell zone in db/db-NS mice ( $n = 6$ ,  $p < 0.05$ ; Fig. 4d, 4e). After si-Rspo3 administration in db/db-NS mice, the high Lgr5 expression was inhibited and the expansion expression of Lgr5 + stem cell zone was reduced by RT-qPCR, Western blot and Immunohistochemistry analysis ( $n = 6$ ,  $p < 0.05$ ; Fig. 4a-4e). Together, these data indicate that Rspo3 is a major determinant of Lgr5 + stem cell identity upon DM state.

### **MiRNA expression profiles were evaluated in IECs of DM state**

To gain a broader view of how Rspo3 was upregulated in IECs of DM state, we performed microarray analysis. Microarray analysis was used to evaluate miRNA expression profiles, and hierarchical clustering identified 14 miRNAs were downregulated in IECs of db/db mice compared to db/+ mice (Fig. 5a; Table S1). Among these miRNAs, miRNA-380-5p, which may target Rspo3, was considered to be a candidate for further investigation by an analysis of the publicly available algorithms (TargetScan, [www.targetscan.org](http://www.targetscan.org); miRanda, [www.microrna.org](http://www.microrna.org); Fig. 5b). RT-qPCR further revealed that miR-380-5p expression in IECs from db/db mice was significantly downregulated compared to db/+ mice ( $n = 6$ ,  $P < 0.05$ ; Fig. 5c). Meantime, in situ hybridization of a DIG-labeled LNA-miR-380-5p probe showed that miR-380-5p was predominantly localized in the stromal compartment that surrounds the crypt base ( $n = 6$ ,  $P < 0.05$ ; Fig. 5d). These results implied that expression and location of miR-380-5p might explain abnormal differentiation of IECs in DM mice.

### **MiR-380-5p regulates abnormal differentiation of IECs by Rspo3 in DM state**

The dual-luciferase reporter assay demonstrated that luciferase expression in 293T cells cotransfected with miR-380-5p mimic and the Rspo3-3'-UTR-wnt plasmid resulted in a significant decrease in luciferase activity ( $n = 6$ ,  $p < 0.05$ ; Fig. 6a). The luciferase activity of the Rspo3-3'-UTR-mut plasmid was not affected by miR-380-5p mimics ( $n = 6$ ,  $p > 0.05$ ; Fig. 6a). These data indicate that miR-380-5p mimic specifically targeted the 3'-UTR of Rspo3, and downregulate expression of the downstream reporter gene. AgomiR-380-5p administration in db/db mice, the overexpression level of Rspo3 and Lgr5 was reduced to normalized by Western blot ( $n = 6$ ,  $p < 0.05$ ; Fig. 6b, 6c). Interestingly, RT-qPCR showed a substantial increased mRNA expression of Sl, Tff3 and Lyz1 and decreased ChgA mRNA expression in db/db mice, that was rescued by administration of agomiR-380-5p ( $n = 6$ ,  $p < 0.05$ ; Fig. 6d). Meanwhile, Sl, Tff3 and Lyz1 protein overexpression fairly decreased and close to the levels seen in db/+ mice through agomiR-380-5p administration ( $n = 6$ ,  $p < 0.05$ ; Fig. 6e, 6f). Furthermore, downregulated ChgA protein expression

was partially normalized after agomiR-380-5p administration compared with db/+ mice ( $n = 6$ ,  $p < 0.05$ ; Fig. 6e, 6f).

## Discussion

DM complications affecting the gastrointestinal tract have already taken more and more attention. And we most focus primarily clinical with the emphasis on the major symptoms involved: diarrhea, constipation and anal sphincter incontinence. In fact, before the above symptoms appear, the intestinal epithelium has already undergone abnormal proliferation and differentiation. The aim of this study was to evaluate abnormal differentiation of IECs in db/db state. In this study, we found that the numbers of SI-, Tff3-, and Lyz1-positive cells in db/db mice were significantly increased, and the decreased numbers of ChgA-positive cells. This was consistent with the direction of the abnormal differentiation of intestinal epithelium in our previous study about Streptozocin (STZ)-induced DM mice model [15]. As we all know, patients with type 1 diabetes and type 2 diabetes are different in etiology, pathogenesis and clinical manifestations. STZ-induced DM mice are often considered as a type 1 diabetes model; however, db/db mice are often considered as a type 2 diabetes model. In this study, it is found that they have the same abnormal differentiation direction of intestinal epithelium at the beginning of DE, but whether it is always the same, we need to further study.

To continue our research, elucidation of the molecular mechanisms that regulate differentiation of IECs, function would be crucial for understanding of intestinal disease pathogenesis in DM state. IESCs rapidly proliferate and differentiate into mature epithelial cells to maintain the intestinal integrity. Lgr5 + crypt cells, IESCs, residing in the crypts are critical for the continual self-renewal and thought to be dispensable for small intestinal (SI) homeostasis [19]. In our study, we found that Lgr5 had expression was highly and had expansion expression of Lgr5 + stem cell zone in db/db mice than those in db/+ mice, and these findings tell us the main reason for abnormal differentiation of IECs in DM state.

In our previous research, we found that the Wnt/ $\beta$ -catenin signaling pathway was continuously activated in IECs of DM mice [14], and the reason why Wnt/ $\beta$ -catenin pathway continuously was activated, and still need further study. In IESCs, the Wnt pathway is essential for intestinal crypt formation and renewal, whereas Rspo-mediated signalling mainly affects ISC numbers [20]. All Rspos have the capacity to induce crypt cell renewal and  $\beta$ -catenin activation [21]. In most previous studies, the knockout RSPO3 model found that RSPO3 is an indispensable factor for the regeneration of intestinal epithelial stem cells [22, 23]. However, in the study model of RSPO3 overexpression, it can cause the occurrence and development of colon cancer by activating the excessive activation of the WNT pathway [24]. In this study, we first found that RSPO3 were also significantly upregulated in the IECs of DM state among RSPO family (RSPO1-4). And, we found that Rspo3 is a major determinant of Lgr5 + stem cell identity upon DM state. Furthermore, the results showed that the numbers of SI-, Tff3-, and Lyz1-positive cells were significantly decreased, and the decreased numbers of ChgA-positive cells observed in db/db mice were normalized after si-Rspo3 administration. These data imply that abnormal differentiation of IECs in DM state is associated with overexpressed Rspo3.

Given the crucial roles in differentiation in IECs, examination of Rspo3 mechanism has provided new insight into the regulatory roles in stem cell behavior. Many studies have demonstrated miRNAs take part roles in differentiation of IECs in the mouse [14, 25, 26]. Through miRNA expression profiles, bioinformatic analysis, and RT-qPCR, we noticed a miRNA, miR-380-5p, which was downregulated in IECs tissues. In addition, by an in situ hybridization of a DIG-labeled LNA-miR-380-5p probe, we found that distribution of miR-380-5p is consistent with Rspo3. MiR-380-5p has been found to be able to regulate the development of different tumors [27, 28]. However, under diabetic conditions, whether miR-380-5p also has its function on differentiation of IECs needs to be clarified. In this study, Luciferase analysis showed that miR-380-5p targeted the Rspo3 gene, and downregulate expression of the downstream reporter gene. Given the common target identified in this work, it is interesting for further studies to determine the extent to which the functions of miR-380-5p in abnormal differentiation of IECs.

Numerous studies have shown that miRNAs can improve intestinal function by participating in the differentiation of cell populations in the intestine [29]. MiR-30 family controls differentiation of IECs models by directing a broad gene expression program that includes SOX9 and the ubiquitin ligase pathway [30]. However, in DM state, there are few studies on whether miRNA regulates the abnormal differentiation of intestinal epithelium and it needs to be confirmed by this study. In this study, numbers of SI, Tff3 and Lyz1 positive cells were significantly lower, and the reduced number of ChgA-positive cells seen in db/db mice was normalized after agomiR-380-5p administration. These results imply that miR-380-5p regulates abnormal differentiation of IECs by Rspo3 in DM state.

## Conclusions

In conclusion, this study provides new evidence that Rspo3 plays a significant role in regulating differentiation in the IECs of DM state. Further analyses Rspo3 is a major determinant of Lgr5 + stem cell identity upon DM state. Decreased expression of miR-380-5p appears to be a key player in this pathological process by targeting the Rspo3.

## Abbreviations

DM, diabetes mellitus; DE, diabetic enteropathy; Rspo R-spondin; miRNA, microRNA; mRNA, messenger RNA; IECs, intestinal epithelial cells; IESCs, intestinal epithelial stem cells; qPCR, quantitative polymerase chain reaction; UTR, untranslated region;

## Declarations

### Acknowledgements

All authors confirmed and supported this study.

### Authors' contributions

STD performed the scientific design, analyzed all the experiments, and drafted the manuscript. STD and HY performed the scientific design and revised the manuscript. HY, SXG, JYP, and CL performed the experiments and critically revised the manuscript; STD, HY, SXG, and CL contributed to the data and statistical analyses.

## **Funding**

This study was supported by the National Natural Science Foundation of China (grant no. 81800461).

## **Availability of data and materials**

All data generated or analyzed during this study are included in this published article.

## **Ethics approval and consent to participate**

The care and use of laboratory animals were approved by Model Animal Research Center of Nanjing University (NO.n45312453) and Animal Use and Care Committee of Qingdao University.

## **Consent for publication**

Not applicable.

## **Competing interests**

The authors declare that they have no competing interests.

## **References**

1. Ergun-Longmire B, et al. Diabetes education in pediatrics: How to survive diabetes. *Dis Mon.* 2021;101153.
2. Prasun P. Role of mitochondria in pathogenesis of type 2 diabetes mellitus. *J Diabetes Metab Disord.* 2020;19:2017-22.
3. D'Addio F, Fiorina P. Type 1 Diabetes and Dysfunctional Intestinal Homeostasis. *Trends Endocrinol Metab.* 2016;27:493-503.
4. Shan TD, Tian ZB, Jiang YP. Downregulation of lncRNA MALAT1 suppresses abnormal proliferation of small intestinal epithelial stem cells through miR-129-5p expression in diabetic mice. *Int J Mol Med.* 2020;45:1250-60.
5. de Kort S, et al. Diabetes mellitus, genetic variants in the insulin-like growth factor pathway and colorectal cancer risk. *Int J Cancer.* 2019;145:1774-81.
6. Wang X, et al. Insulin resistance in vascular endothelial cells promotes intestinal tumour formation. *Oncogene.* 2017;36:4987-96.

7. Sei Y, Feng J, Chow CC, Wank SA. Asymmetric cell division-dominant neutral drift model for normal intestinal stem cell homeostasis. *Am J Physiol Gastrointest Liver Physiol*. 2019;316:G64-G74.
8. Powell AE, et al. Inducible loss of one Apc allele in Lrig1-expressing progenitor cells results in multiple distal colonic tumors with features of familial adenomatous polyposis. *Am J Physiol Gastrointest Liver Physiol*. 2014;307:G16-23.
9. de Lau WB, Snel B, Clevers HC. The R-spondin protein family. *Genome Biol*. 2012;13:242.
10. Mah AT, Yan KS, Kuo CJ. Wnt pathway regulation of intestinal stem cells. *J Physiol*. 2016;594:4837-47.
11. Bracken CP, Scott HS, Goodall GJ. A network-biology perspective of microRNA function and dysfunction in cancer. *Nat Rev Genet*. 2016;17:719-32.
12. Huang CZ, et al. Sox9 transcriptionally regulates Wnt signaling in intestinal epithelial stem cells in hypomethylated crypts in the diabetic state. *Stem Cell Res Ther*. 2017;8:60.
13. Livak KJ, Schmittgen TD. Analysis of relative gene expression data using real-time quantitative PCR and the 2(-Delta Delta C(T)) Method. *Methods*. 2001;25:402-8.
14. Shan TD, et al. Knockdown of lncRNA H19 inhibits abnormal differentiation of small intestinal epithelial cells in diabetic mice. *J Cell Physiol*. 201;234:837-48.
15. Shan TD, et al. miRNA-30e regulates abnormal differentiation of small intestinal epithelial cells in diabetic mice by downregulating Dll4 expression. *Cell Prolif*. 2016;49:102-14.
16. Gracz AD, Ramalingam S, Magness ST. Sox9 expression marks a subset of CD24-expressing small intestine epithelial stem cells that form organoids in vitro. *Am J Physiol Gastrointest Liver Physiol*. 2010;298:G590-600.
17. Tay Y, et al. Coding-independent regulation of the tumor suppressor PTEN by competing endogenous mRNAs. *Cell*. 2011;147:344-57.
18. Cesana M, et al. A long noncoding RNA controls muscle differentiation by functioning as a competing endogenous RNA. *Cell*. 2011;147:358-69.
19. Tan SH, et al. A constant pool of Lgr5+ intestinal stem cells is required for intestinal homeostasis. *Cell Rep*. 2021;34:108633.
20. Kriz V, Korinek V. Wnt, RSPO and Hippo Signalling in the Intestine and Intestinal Stem Cells. *Genes (Basel)*. 2018;9:20.
21. Kim KA, et al. R-Spondin proteins: a novel link to beta-catenin activation. *Cell Cycle*. 2006;5:23-6.
22. Harnack C, et al. R-spondin 3 promotes stem cell recovery and epithelial regeneration in the colon. *Nat Commun*. 2019;10:4368.
23. Greicius G, et al. PDGFR $\alpha$ + pericryptal stromal cells are the critical source of Wnts and RSPO3 for murine intestinal stem cells in vivo. *Proc Natl Acad Sci U S A*. 2018;115:E3173-81.
24. Hilkens J, et al. RSPO3 expands intestinal stem cell and niche compartments and drives tumorigenesis. *Gut*. 2017;66:1095-105.

25. McKenna LB, et al. MicroRNAs control intestinal epithelial differentiation, architecture, and barrier function. *Gastroenterology*. 2010;139:1654-64, 1664.e1.
26. Chivukula RR, et al. An essential mesenchymal function for miR-143/145 in intestinal epithelial regeneration. *Cell*. 2014;157:1104-16.
27. Cimino-Reale G, et al. miR-380-5p-mediated repression of TEP1 and TSPYL5 interferes with telomerase activity and favours the emergence of an "ALT-like" phenotype in diffuse malignant peritoneal mesothelioma cells. *Hematol Oncol*. 2017;10:140.
28. Swarbrick A, et al. miR-380-5p represses p53 to control cellular survival and is associated with poor outcome in MYCN-amplified neuroblastoma. *Nat Med*. 2010;16:1134-40.
29. Ding S, et al. MicroRNA Determines the Fate of Intestinal Epithelial Cell Differentiation and Regulates Intestinal Diseases. *Curr Protein Pept Sci*. 2019;20:666-673.
30. Peck BC, et al. miR-30 Family Controls Proliferation and Differentiation of Intestinal Epithelial Cell Models by Directing a Broad Gene Expression Program That Includes SOX9 and the Ubiquitin Ligase Pathway. *J Biol Chem*. 2016;291:15975-84.

## Figures

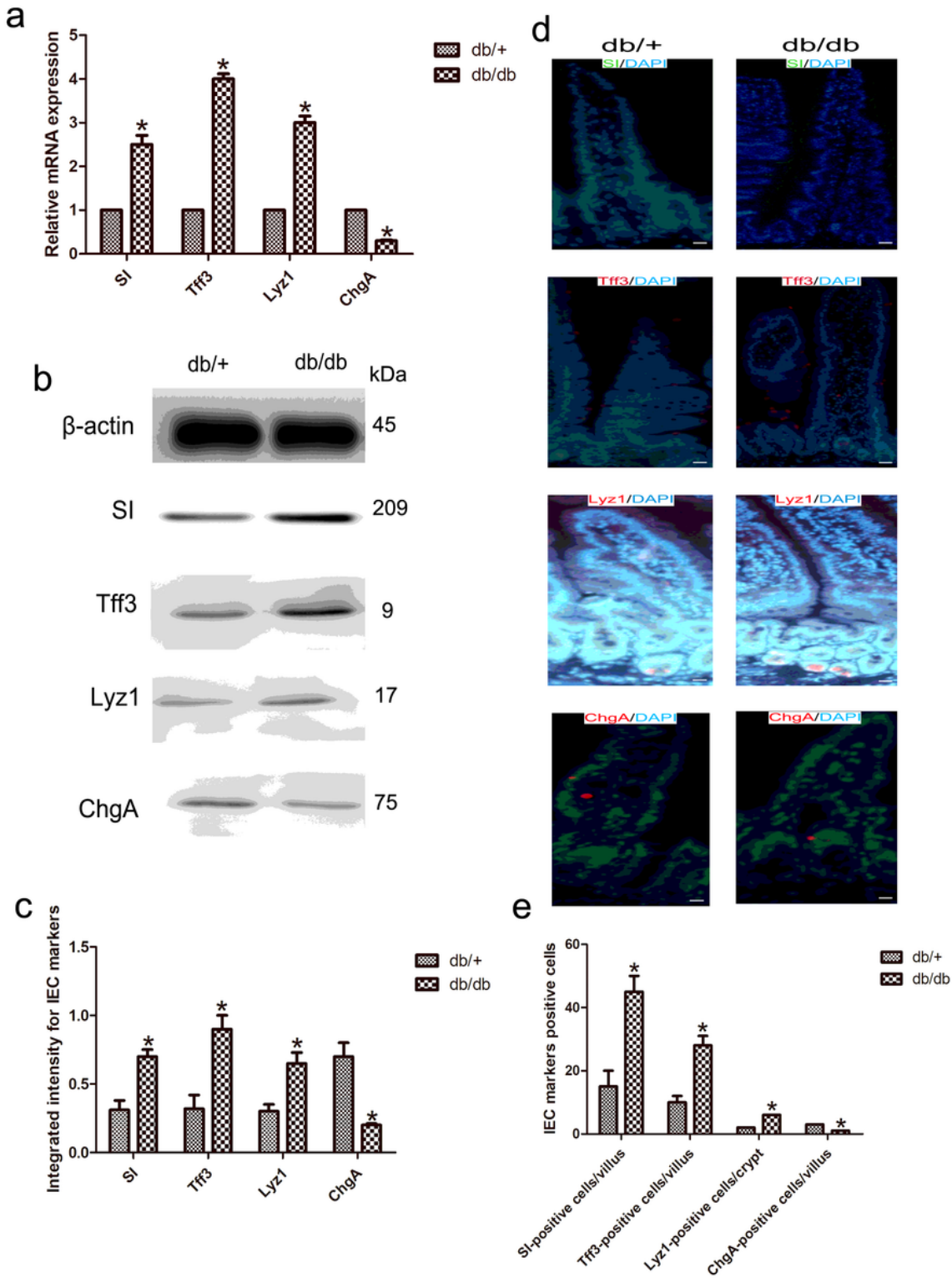


**Figure 1**

Abnormal differentiation of IECs in DM state. (a) The mRNA expression level of SI, Tff3, Lyz1 and ChgA in the IECs of the db/db group and db/+ group. (b-c) Western blot analysis showed the protein expression of SI, Tff3, Lyz1 and ChgA in two groups. (d-e) Immunohistochemistry shows the numbers of SI-, Tff3-, Lyz1- and ChgA-positive cells. Scale bar, 50  $\mu$ m; mean  $\pm$  SD, n = 6; \*P<0.05.

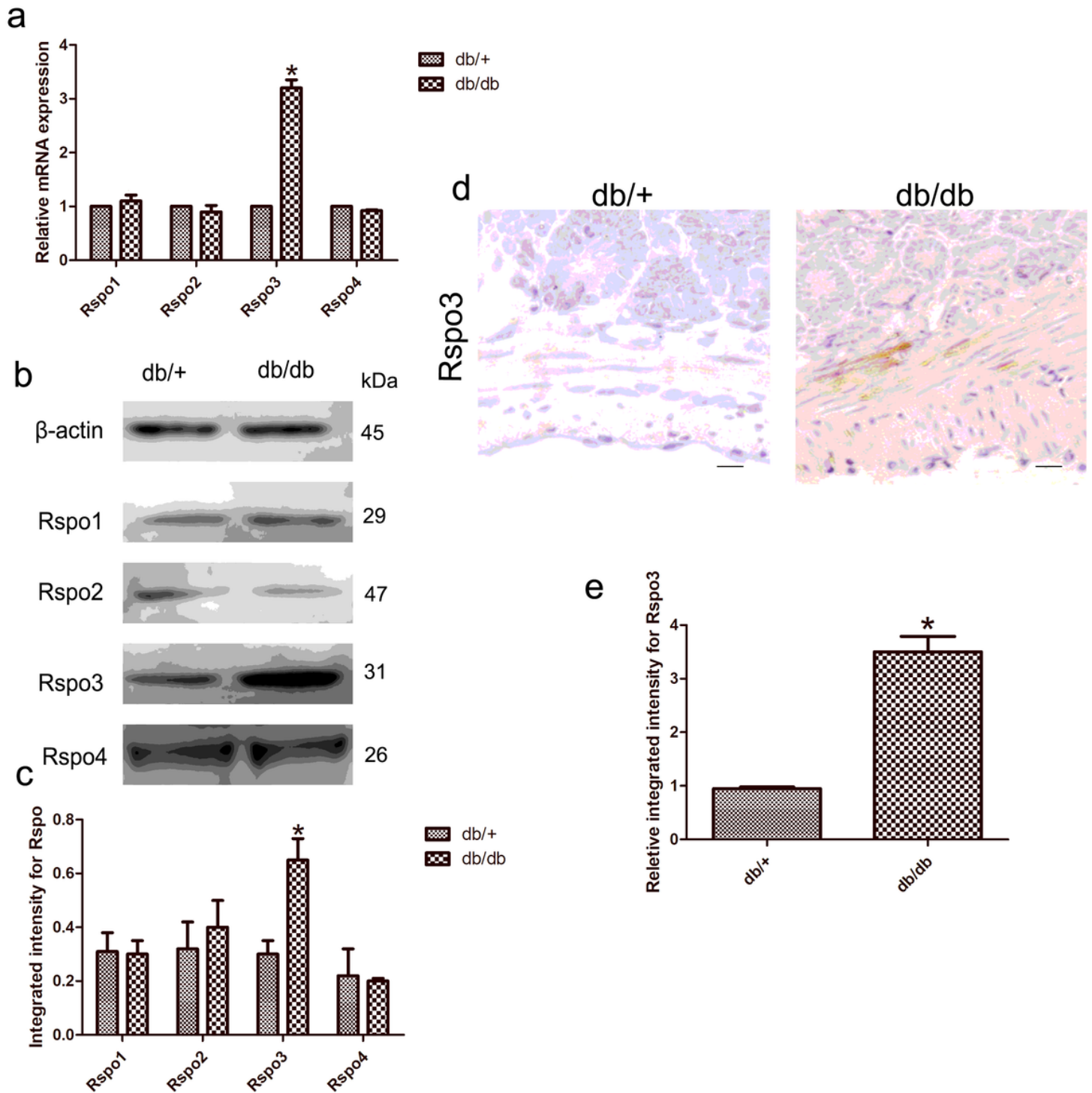


**Figure 2**

The expression of Rspo3 in the IECs of DM state. (a) RT-qPCR analysis showed that the mRNA expression of Rspos in the IECs of db/db mice and db/+ mice. (b-c) Rspo3 protein levels were also significantly upregulated in the IECs of db/db mice. (d-e) Immunohistochemistry showed that Rspo3 expression localized surrounds the crypt base. Scale bar, 50  $\mu$ m; mean  $\pm$  SD, n = 6; \*P<0.05.

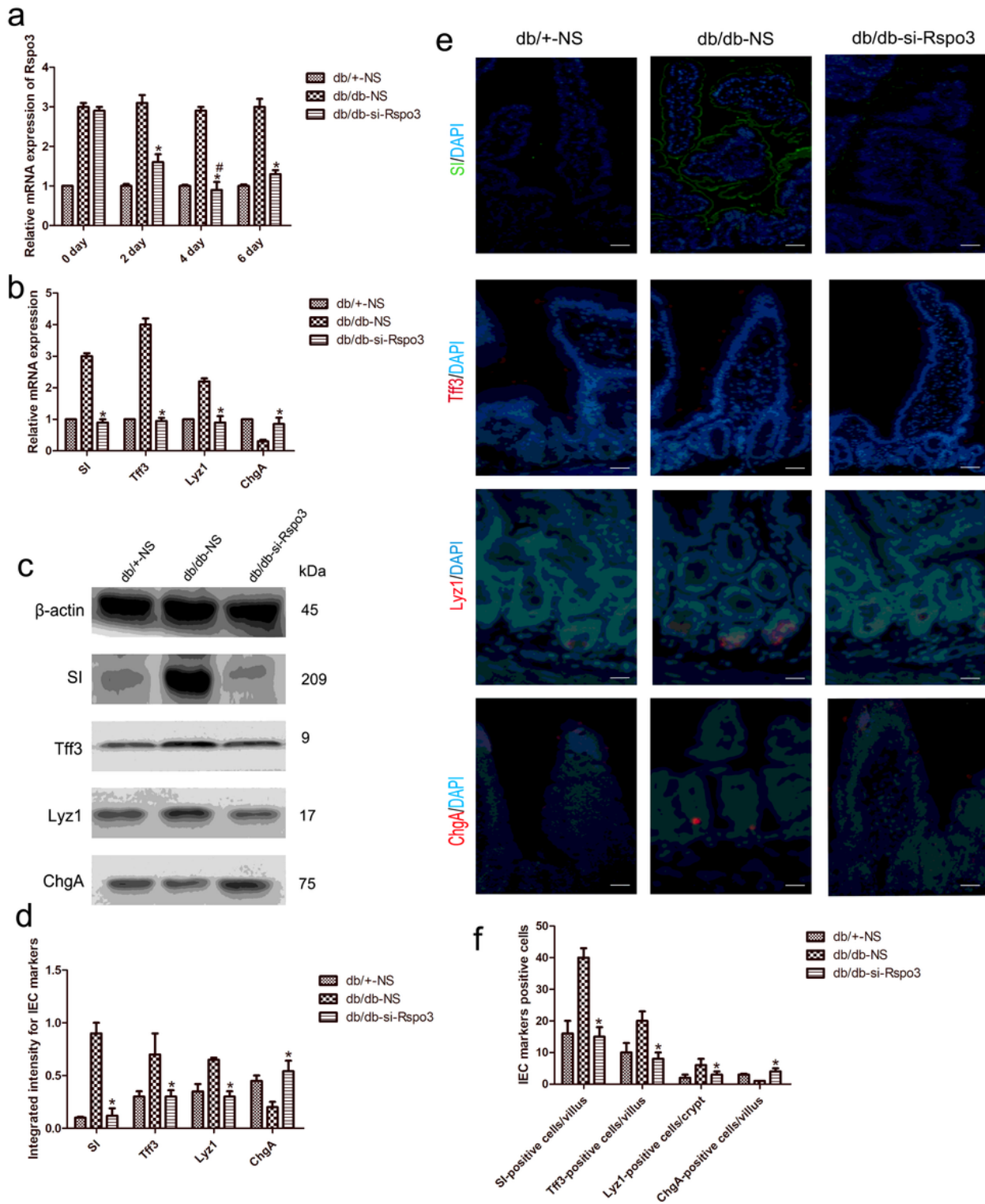


**Figure 3**

Abnormal differentiation of IECs in DM state is associated with overexpressed Rspo3. (a) The knockdown efficiencies in vitro after transfection of siRNAs in DM. (b) The mRNA expression of SI, Tff3, Lyz1 and ChgA after si-Rspo3 administration in the IECs of db/db mice. (c-d) Western blot showed the protein expression of SI, Tff3, Lyz1 and ChgA in si-Rspo3 administration db/db mice. (e-f) The numbers of SI,

Tff3-, Lyz1-, and ChgA-positive cells in si-Rspo3 administration db/db mice. Scale bar, 50  $\mu$ m; mean  $\pm$  SD, n = 6; \*P<0.05 vs db/+NS.

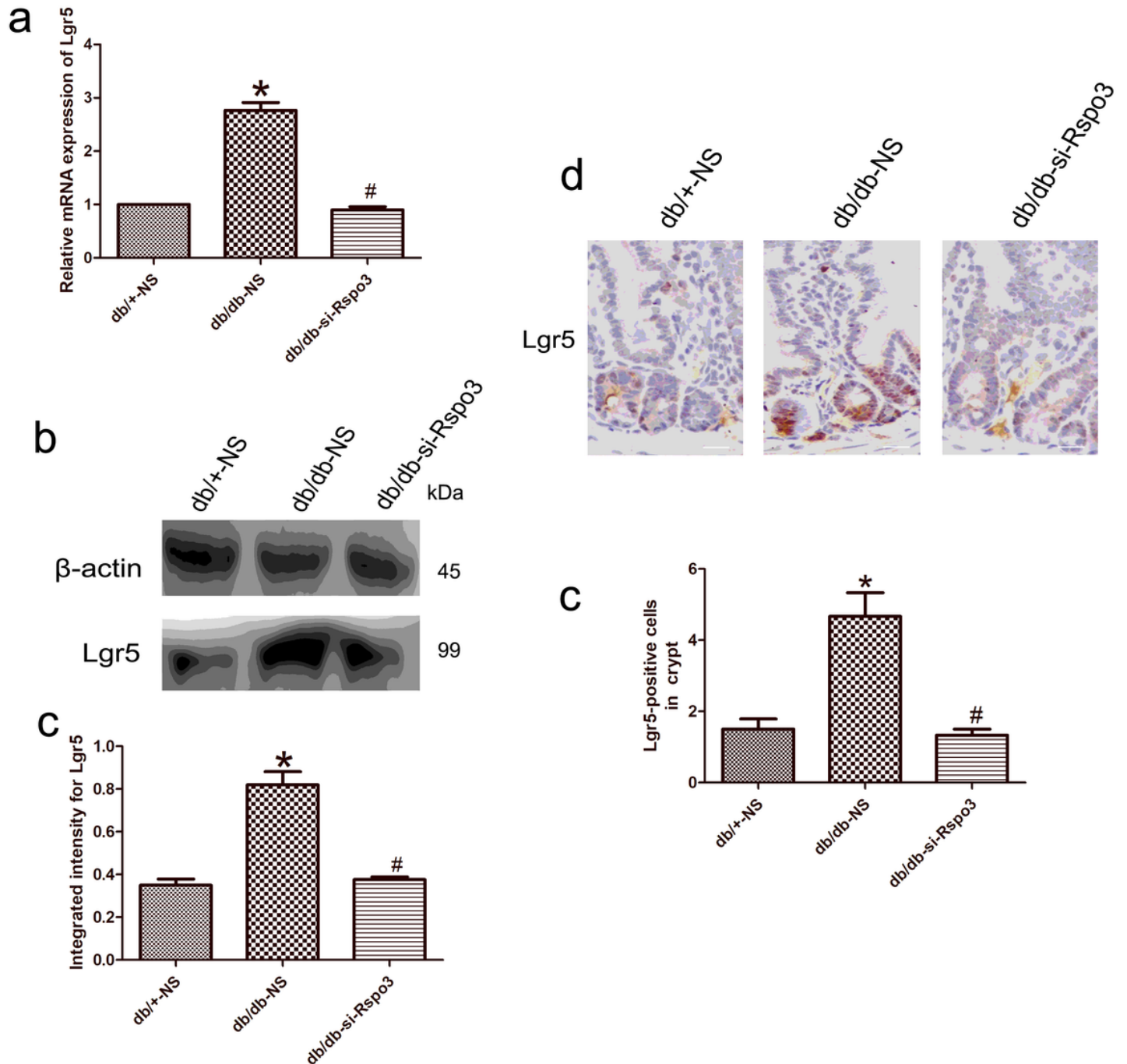


**Figure 4**

Rspo3 expands Lgr5+ stem cells in DM state. (a) RT-qPCR revealed that Lgr5 in db/db-NS mice showed the higher expression compared with db/+NS mice, and high Lgr5 expression was decreased after si-Rspo3 administration. (b-c) Western blot showed Lgr5 protein levels were upregulated, the downregulated in si-Rspo3 administration db/db mice. (d-e) Immunohistochemistry was found that Lgr5 expression was predominantly localized in crypt of IECs and had expansion expression of Lgr5+ stem cell zone in db/db-NS mice). After si-Rspo3 administration in db/db-NS mice, the high Lgr5 expression was inhibited and the

expansion expression of Lgr5+ stem cell zone was reduced. Scale bar, 50  $\mu$ m; mean  $\pm$  SD, n = 6; \*P<0.05 vs db/+NS; #P<0.05 vs db/db-NS.

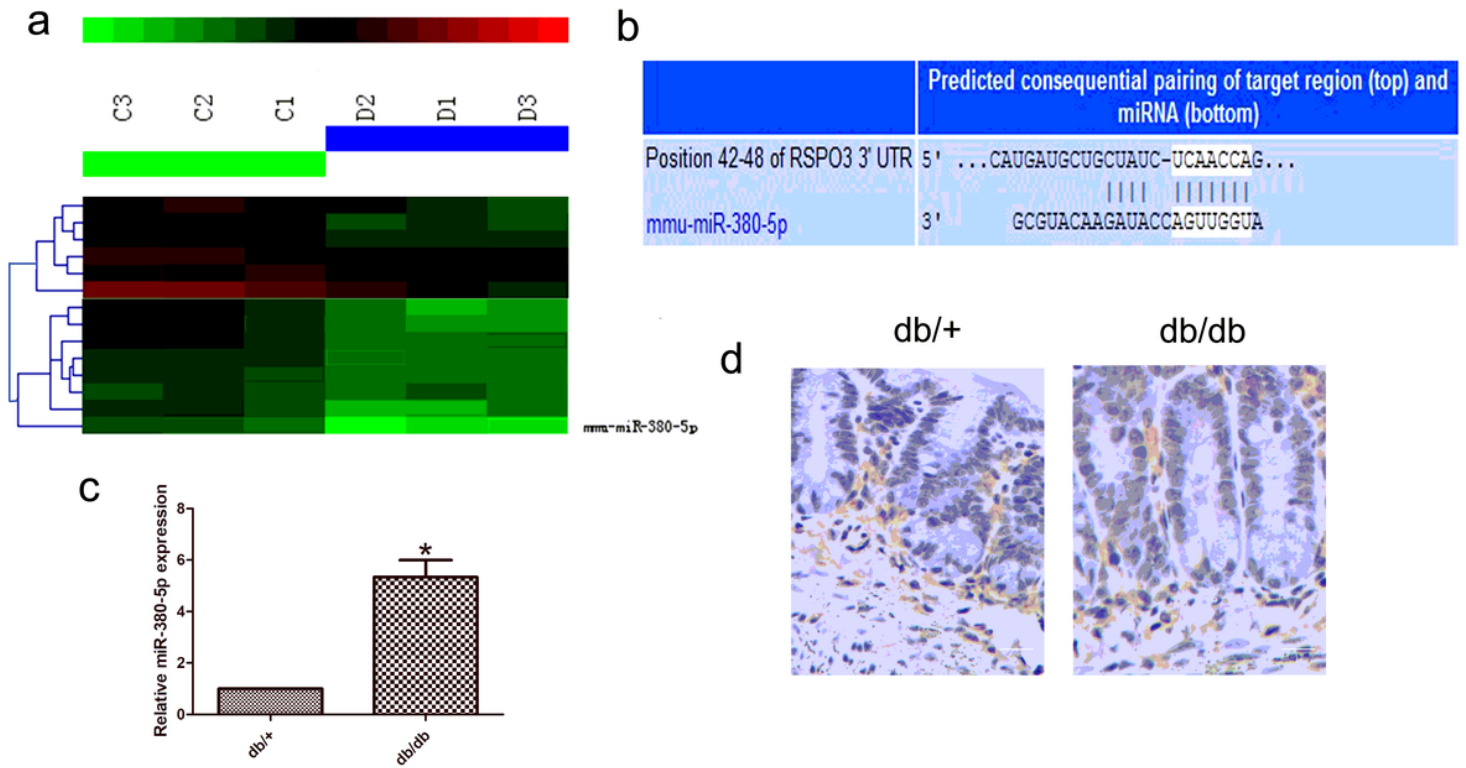


**Figure 5**

MiRNA expression profiles were evaluated in IECs of DM state. (a) Microarray analysis was used to evaluate miRNA expression profiles in db/db mice. (b) Rspo3 target Rspo3 by an analysis of the publicly available algorithms. (c) RT-qPCR revealed that miR-380-5p expression in IECs was downregulated in db/db mice. (d) In situ hybridization of a DIG-labeled LNA-miR-380-5p probe showed that miR-380-5p was predominantly localized surrounds the crypt base. Scale bar, 50  $\mu$ m; mean  $\pm$  SD, n = 6; \*P<0.05.

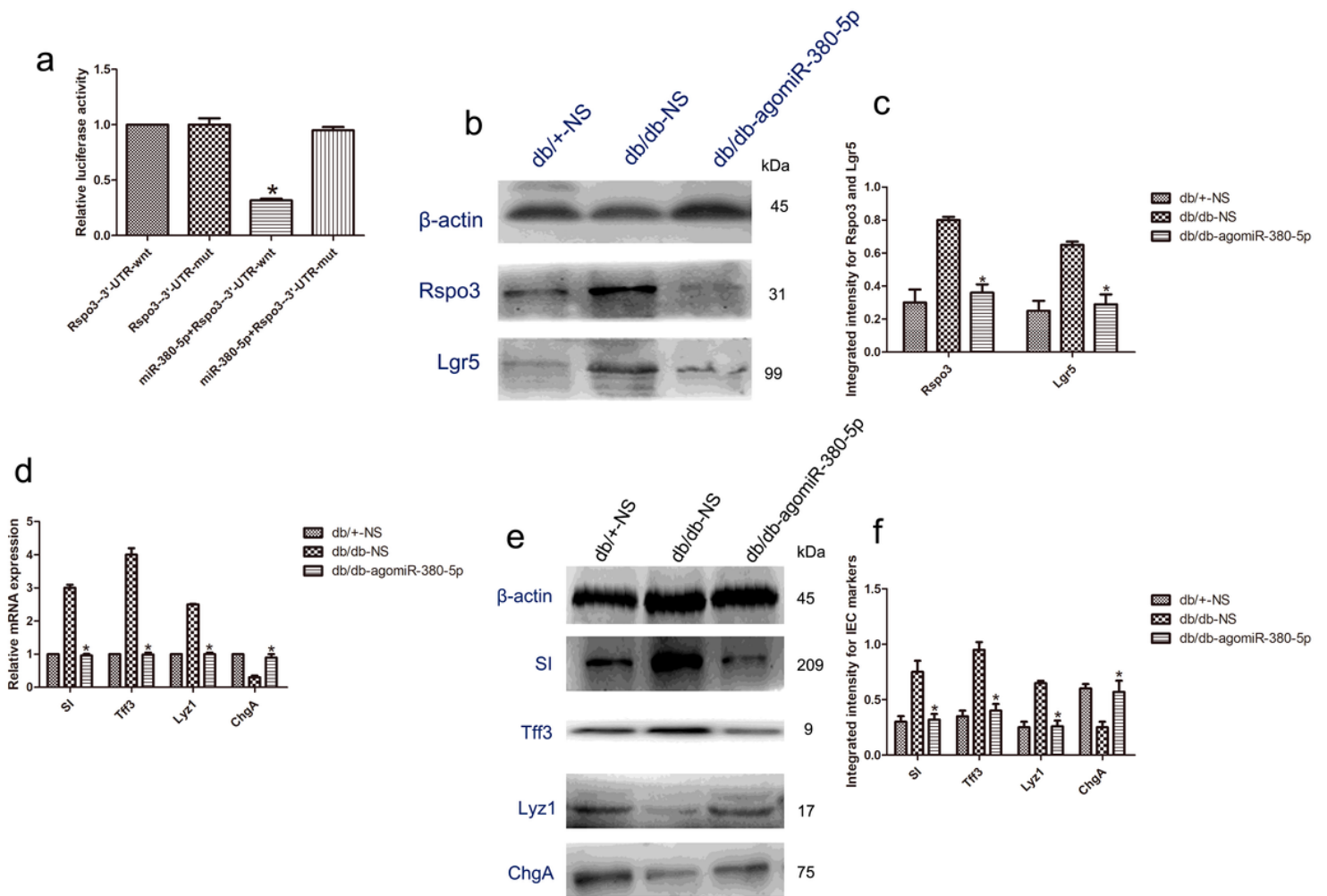


**Figure 6**

MiR-380-5p regulates abnormal differentiation of IECs by Rspo3 in DM state. (a) The dual-luciferase reporter assay demonstrated that miR-380-5p mimic and the Rspo3-3'-UTR-wnt plasmid caused a significant decrease in luciferase activity. (b-c) AgomiR-380-5p administration in db/db mice, the overexpression level of Rspo3 and Lgr5 was reduced after gomiR-380-5p administration in db/db mice by Western blot. (d) RT-qPCR showed a substantial increased mRNA expression of SI, Tff3 and Lyz1 and decreased ChgA mRNA expression in db/db mice, that was rescued by administration of agomiR-380-5p. (e-f) SI, Tff3 and Lyz1 protein overexpression fairly decreased and close to the levels seen in db/+ mice through agomiR-380-5p administration, and downregulated ChgA protein expression was partially normalized after agomiR-380-5p administration compared with db/+ mice. mean  $\pm$  SD, n = 6; \*P<0.05 vs db/+NS; #P<0.05 vs db/db-NS.

## Supplementary Files

This is a list of supplementary files associated with this preprint. Click to download.

- [SupplementaryMaterial.docx](#)